NASA/TM—2012-217737

Utilization of the Generalized Method of Cells to Analyze the Deformation Response of Laminated Ceramic Matrix Composites

Robert K. Goldberg
Glenn Research Center, Cleveland, Ohio

October 2012

NASA STI Program . . . in Profile

Since its founding, NASA has been dedicated to the advancement of aeronautics and space science. The NASA Scientific and Technical Information (STI) program plays a key part in helping NASA maintain this important role.

The NASA STI Program operates under the auspices of the Agency Chief Information Officer. It collects, organizes, provides for archiving, and disseminates NASA's STI. The NASA STI program provides access to the NASA Aeronautics and Space Database and its public interface, the NASA Technical Reports Server, thus providing one of the largest collections of aeronautical and space science STI in the world. Results are published in both non-NASA channels and by NASA in the NASA STI Report Series, which includes the following report types:

- TECHNICAL PUBLICATION. Reports of completed research or a major significant phase of research that present the results of NASA programs and include extensive data or theoretical analysis. Includes compilations of significant scientific and technical data and information deemed to be of continuing reference value. NASA counterpart of peer-reviewed formal professional papers but has less stringent limitations on manuscript length and extent of graphic presentations.

- TECHNICAL MEMORANDUM. Scientific and technical findings that are preliminary or of specialized interest, e.g., quick release reports, working papers, and bibliographies that contain minimal annotation. Does not contain extensive analysis.

- CONTRACTOR REPORT. Scientific and technical findings by NASA-sponsored contractors and grantees.

- CONFERENCE PUBLICATION. Collected papers from scientific and technical conferences, symposia, seminars, or other meetings sponsored or cosponsored by NASA.

- SPECIAL PUBLICATION. Scientific, technical, or historical information from NASA programs, projects, and missions, often concerned with subjects having substantial public interest.

- TECHNICAL TRANSLATION. English-language translations of foreign scientific and technical material pertinent to NASA's mission.

Specialized services also include creating custom thesauri, building customized databases, organizing and publishing research results.

For more information about the NASA STI program, see the following:

- Access the NASA STI program home page at *http://www.sti.nasa.gov*

- E-mail your question to *help@sti.nasa.gov*

- Fax your question to the NASA STI Information Desk at 443–757–5803

- Phone the NASA STI Information Desk at 443–757–5802

- Write to:
  STI Information Desk
  NASA Center for AeroSpace Information
  7115 Standard Drive
  Hanover, MD 21076–1320

NASA/TM—2012-217737

Utilization of the Generalized Method of Cells to Analyze the Deformation Response of Laminated Ceramic Matrix Composites

Robert K. Goldberg
Glenn Research Center, Cleveland, Ohio

Prepared for the
27th Technical Conference
sponsored by the American Society for Composites
Arlington, Texas, October 1–3, 2012

National Aeronautics and
Space Administration

Glenn Research Center
Cleveland, Ohio 44135

October 2012

This work was sponsored by the Fundamental Aeronautics Program at the NASA Glenn Research Center.

Level of Review: This material has been technically reviewed by technical management.

Available from

NASA Center for Aerospace Information
7115 Standard Drive
Hanover, MD 21076–1320

National Technical Information Service
5301 Shawnee Road
Alexandria, VA 22312

Available electronically at http://www.sti.nasa.gov

Utilization of the Generalized Method of Cells to Analyze the Deformation Response of Laminated Ceramic Matrix Composites

Robert K. Goldberg
National Aeronautics and Space Administration
Glenn Research Center
Cleveland, Ohio 44135

Abstract

In order to practically utilize ceramic matrix composites in aircraft engine components, robust analysis tools are required that can simulate the material response in a computationally efficient manner. The MAC/GMC software developed at NASA Glenn Research Center, based on the Generalized Method of Cells micromechanics method, has the potential to meet this need. Utilizing MAC/GMC, the effective stiffness properties, proportional limit stress and ultimate strength can be predicted based on the properties and response of the individual constituents. In this paper, the effective stiffness and strength properties for a representative laminated ceramic matrix composite with a large diameter fiber are predicted for a variety of fiber orientation angles and laminate orientations. As part of the analytical study, methods to determine the in-situ stiffness and strength properties of the constituents required to appropriately simulate the effective composite response are developed. The stiffness properties of the representative composite have been adequately predicted for all of the fiber orientations and laminate configurations examined in this study. The proportional limit stresses and strains and ultimate stresses and strains were predicted with varying levels of accuracy, depending on the laminate orientation. However, for the cases where the predictions did not have the desired level of accuracy, the specific issues related to the micromechanics theory were identified which could lead to difficulties that were encountered that could be addressed in future work.

Introduction

Ceramic matrix composites (CMCs) are being investigated for use in high temperature applications. Potential application areas include hot-section components such as blades, vanes, combustor liners and nozzles, as well as airframe structural components such as wing leading edges. Ceramic matrix composites offer several advantages over monolithic ceramics including higher specific stiffness and strength, lower density, improved toughness and more gradual failure modes. However, in order to practically design components using these materials, robust analysis tools are required that can simulate the material response in a computationally efficient manner. These required design and analysis tools are still under development.

There have been some efforts in the past to predict the effective stiffness properties and strengths of ceramic matrix composites utilizing micromechanics based approaches, in which the properties and response of the individual constituents are utilized to predict the effective properties and response of the overall composite. There are two key effective strength values that are used in the analysis and design of structures utilizing ceramic matrix composites. The first value, the "first matrix cracking stress" or "proportional limit", is defined as the stress level where the stress-strain curves first displays a significant deviation from linearity. This value is particularly important in the design of components constructed using ceramic matrix composites as once matrix cracking takes place oxygen can penetrate into the composite and degrade the material. The second value, the "ultimate strength", has the classical definition of the highest stress level the material can reach under loading. Murthy, et al. (Ref. 1) utilized a simplified micromechanics approach to predict the effective stiffness properties and the stress-strain curves for a

laminated ceramic matrix composite. Through the computed stress-strain curves, the first matrix cracking stress and ultimate strengths were predicted. A maximum stress failure criterion was applied to each constituent, and a progressive failure algorithm was employed to track the evolution of the local failures. Researchers such as Lamon (Ref. 2) have utilized a combination of fracture mechanics and Weibull statistics to predict the first matrix cracking stress and ultimate strength of ceramic matrix composites based on the properties of the constituents. Mital, et al. (Ref. 3) predicted the effective stiffness properties of a representative woven CMC utilizing a variety of micromechanics approaches, including the Generalized Method of Cells, finite element analyses and several other analytical micromechanics approaches. Liu and Arnold (Ref. 4) utilized a multiscale expansion of the Generalized Method of Cells along with a bilinear matrix damage model to predict the stress-strain response (including nonlinearity) of a woven ceramic matrix composite.

As implied by the discussion above, the Generalized Method of Cells micromechanics approach (Refs. 5 and 6) has the potential to serve as a valuable tool to predict the effective stiffness and strength properties of ceramic matrix composites in a computationally efficient manner given the properties of the constituents. One key challenge in utilizing micromechanics approaches in the analysis of ceramic matrix composites is that oftentimes the in-situ properties of the constituents, particularly the fiber coating (which forms the fiber/matrix interface, is a significant percentage of the fiber diameter, and contributes significantly to the effective response of the composite) and the matrix are difficult, if not impossible, to obtain experimentally due to effects such as voids and residual stresses. Therefore, systematic methods to characterize the required constituent properties based on available data for the overall composite need to be developed.

The goal of the current paper is to evaluate the capability of the Generalized Method of Cells and its implementation within the NASA Glenn developed analysis code MAC/GMC (Ref. 7) to analyze the mechanical response of laminated ceramic matrix composites, including the determination of effective stiffness and strength values, along with the generation of effective stress-strain curves. A specific laminated ceramic matrix composite, SiC/RBSN, was analyzed due to the fact that significant experimental and analytical studies of this material have taken place at NASA Glenn (Refs. 1 and 8), leading to a reasonable availability of constituent and composite data. First, the Generalized Method of Cells (GMC) micromechanics method will be described, with a particular focus on those features of the method that are important in the analysis of ceramic matrix composites. Next, the specific laminated ceramic matrix composite that is analyzed in this paper will be described, along with basic setup of the composite model. The procedures that were used to correlate the constituent properties required for the analysis will be described. Note that in this paper the focus will be on the analysis of laminated ceramic matrix composites, the procedures could most likely also be generalized for the case of woven composites. Next, the effective stiffness properties, first matrix cracking stress and ultimate strength will be computed for the representative ceramic matrix composite. Unidirectional plies loaded both along the fiber direction as well as at multiple off-axis angles will be analyzed, as well as representative cross-ply and angle-ply laminates. Beside the computation of the effective stiffness and strength properties, a discussion of the ability of the GMC micromechanics method to identify the specific local damage mechanisms that contribute to the key features of the macroscopic deformation response will be explored.

Generalized Method of Cells Micromechanics Method

The Generalized Method of Cells micromechanics approach, which has been implemented within the MAC/GMC software package developed at NASA Glenn Research Center (Ref. 7), is a computationally efficient approach to compute the effective properties and response of a composite composed of an arbitrary number of constituents. In the analysis method, the composite repeating unit cell is divided up into an arbitrary number of subcells, each of which can be composed of a different material. This concept is shown in Figure 1 (Ref. 7) for the case of double periodicity, where the unit cell is divided into N_β by N_γ subcells. For the case of the standard Generalized Method of Cells, each subcell is assumed to have a linear displacement field. A set of displacement and traction (constant stress and strain) continuity

conditions are applied between each of the subcells, which, when appropriately combined with the constitutive equations for each of the subcells, results in a series of algebraic equations that can be solved for the local stresses and strains in each subcell, given the global strains, which makes the method very efficient. The resulting equations can then be manipulated to obtain the effective stiffness properties and global stresses based on the constituent properties and local stresses and strains. An important point to note is that a fundamental limitation of this method (and other efficient micromechanics approaches) is that the normal and shear responses of the material are uncoupled, i.e., if only a normal strain is applied there can be no local shear stresses in any of the subcells, and vice versa.

To compute the initiation and progression of damage, at each load step in an incremental loading process, the total stresses in each of the subcells are computed. A failure criterion is then utilized involving the local stresses and constituent strengths to determine whether or not failure has occurred. In the current version of MAC/GMC, the maximum stress, maximum strain and Tsai-Wu failure criteria are available for use (Ref. 7). If the failure criterion is satisfied (i.e., local failure has occurred) within a subcell, the stiffness of the particular subcell is instantaneously reduced to a negligible value. A revised effective stiffness for the composite is then computed, and the analysis proceeds with the revised stiffness values. Note that for the analyses described in this paper, a purely elastic response of the composite is assumed, so that the current total stress in the composite can be computed by multiplying the current effective stiffness matrix by the current value of the total strains.

Analysis Setup

For the studies conducted and presented in this paper, a laminated ceramic matrix composite composed of silicon carbide SCS-6 fibers (142 μm diameter) in a reaction bonded silicon nitride matrix (SiC/RBSN) was analyzed. As mentioned earlier, this particular composite was chosen as a model material since it has been studied extensively at NASA Glenn Research Center (Refs. 1 and 8) and has been well characterized experimentally and analytically. The fiber has an outer carbon layer, which results in a very weak fiber/matrix interface, with a thickness equal to three percent of the fiber diameter. The nominal fiber volume fraction of the composite is 30 percent. More details of the composite and its fabrication can be found in Bhatt and Phillips (Ref. 8). As described in Bhatt and Phillips (Ref. 8), tensile stress-strain curves were obtained for laminates with $[0°]_8$, $[90°]_8$, $[10°]_8$, $[45°]_8$, $[0°_2/90°_2]_s$ and $[+45_2/-45_2]_s$ ply layups. The $[0°]_8$ and $[0°_2/90°_2]_s$ stress-strain curves displayed a bilinear behavior, with an initial elastic modulus, significant matrix cracking followed by a secondary modulus until the final composite failure. The $[90°]_8$, $[10°]_8$, and $[45°]_8$ laminate stress-strain curves had a linear response until a sudden brittle failure. The failure initiated with fiber/matrix debonding and then proceeded immediately to an ultimate brittle failure (Ref. 8). The $[+45_2/-45_2]_s$ stress-strain curve displayed an initial elastic response followed by matrix damage and a more gradual softening of the stress-strain curve. Note that, even though there is a significant statistical variation in the material response (Ref. 8), and that both the constituent properties and effective response of ceramic matrix composites are known in general to be highly stochastic (Refs. 2 and 4), only deterministic analyses were performed to capture the average, or mean, response of the material. Average values were used for the constituent properties, and the average material effective properties and response were examined and computed. Future efforts will involve adding stochastic/probabilistic methods to the analysis.

The MAC/GMC unit cell that was used for the analysis is shown in Figure 2 (Ref. 7). Note that the unit cell shown is not to scale for this particular problem, but is just a generic depiction of the subcell layout. The interface was modeled as a distinct constituent with a thickness equal to three percent of the fiber diameter, similar to the approach utilized by Murthy, et al. (Ref. 1). This relatively simple unit cell was analyzed in order to provide initial insights into how the micromechanics method is analyzing the physics of the problem. Furthermore, this simplified unit cell is a very efficient model which would be good to use in a multiscale analysis. In future efforts, more complex unit cells that might more realistically represent the composite microstructure and enable the simulation of more complex

deformation and damage mechanisms will be studied. The classical lamination theory module available within MAC/GMC was used to analyze fiber layups with other than a [0°] orientation.

Composite laminates with the orientations that were tested by Bhatt and Phillips (Ref. 8) were examined. The room temperature longitudinal responses of the laminates were computed. The composites were loaded in tension under a strain controlled loading until ultimate failure occurred. As discussed in Murthy, et al. (Ref. 1), to accurately model the progressive damage in the composite, an appropriate cool down has to be applied from an elevated temperature in order to ensure that residual stresses are appropriately accounted for within the material. The process of applying a cool down from an elevated temperature to induce residual stresses was also carried out for this study. As shown in Table 1, for the SiC/RBSN material examined in this study, the coefficient of thermal expansion of the fiber is significantly greater than that of the matrix, leading to significant residual tensile stresses in the matrix after the cool down is applied. Bhatt and Phillips (Ref. 8) describes how the composite is formed by nitriding at a temperature of 1200 °C and is then cooled down to room temperature. However, as discussed in Reference 1, the actual stress-free temperature of the composite can be much lower than the temperature at which the nitration took place. Murthy, et al. (Ref. 1) speculated that at higher temperatures the chemical reactions that formed the composite were still taking place, and therefore the cool down would not apply stresses to the composite. Details on how the stress-free temperature was determined will be described in the next section.

A maximum stress criterion was applied for all of the constituents in the analysis. During a particular load step, if the tensile stress in any direction in a particular subcell exceeded the specified tensile strength, the stiffness of the subcell was set to a negligible value and the analysis continued. Ultimate failure was considered to have occurred when the effective stress level in the composite reached a negligible value due to a sufficient number of subcells having a negligible stiffness.

Characterization of Constituent Properties

Ideally, in a micromechanics analysis, the stiffness properties and ultimate strengths of the individual constituents in the composite could be utilized directly within the analysis to compute the effective properties and response of the material. However, as discussed in Murthy, et al. (Ref. 1), for laminated ceramic matrix composites, such an approach cannot be applied, and the constituent properties need to be correlated based on composite level test data due to the fact that the in-situ properties cannot be determined experimentally. There are two particular material property values which dictate some level of constituent property correlation.

First, the stress-free temperature from which the cool down was initiated had to be determined. The temperature needed to be high enough that the appropriate amount of residual stress was captured. However, the temperature needed to be low enough that failure in the constituents did not take place before the cool down was completed. To determine the correct cool down temperature, the first matrix cracking stress (the point of the deviation from linearity in a stress-strain curve) for [0°] unidirectional laminates was used as the basis of correlation. The internal damage leading to the first matrix cracking stress for a [0°] laminate has been found (Ref. 8) to be primarily driven by significant cracking in the matrix, with little if any contribution from the interface. As a result, given the bulk strength of the matrix (which was determined in Bhatt and Phillips (Ref. 8)), the one variable which affected the value of the first matrix cracking stress was assumed to be the amount of tensile residual stress applied to the matrix, controlled by the stress free temperature. By adjusting the stress free temperature until the computed first matrix cracking stress matched the experimental value, a stress free temperature of 400 °C was determined. Since the residual stresses in the matrix at room temperature were tensile, varying the amount of residual stresses (by adjusting the cool down temperature) would affect the composite first matrix cracking stress (with higher residual stresses leading to higher overall matrix stresses leading to a lower first matrix cracking stress). Therefore, by correlating to the matrix cracking stress the appropriate level of residual stresses were indirectly obtained. This value was purely correlated; future studies need to take

place to determine if this value is realistic. The ultimate strength of the [0°] laminate can be related to the axial failure of the fibers (Ref. 8). Therefore, the axial failure strength of the fibers was correlated using the [0°] laminate ultimate strength, i.e., the failure strength was adjusted until the computed ultimate strength matched the experimental value. The fiber was assumed to be an isotropic material, therefore the transverse strength of the fiber was set equal to the axial strength, and the shear strength of the fiber was set to be the axial strength of the fiber divided by the square root of three (a von Mises type of assumption for an isotropic material (Ref. 9)). The stiffness and thermal expansion properties of the fiber given by Murthy, et al. (Ref. 1) were used. As mentioned above, the axial and transverse strengths of the matrix (assuming an isotropic material) were set equal to the bulk matrix strength determined by Bhatt and Phillips (Ref. 8). The shear strength of the matrix was set equal to the axial strength divided by the square root of three (a von Mises type of assumption (Ref. 9)). The matrix stiffness and thermal expansion properties given by Murthy, et al. (Ref. 1) were used. All of the stiffness and strength property values for the fiber and matrix are given in Table 1.

The second aspect of the constituent material property characterization process that required correlation based on composite data was the stiffness and strength of the fiber/matrix interface. The interface plays a key role in the response of ceramic matrix composites. It is generally very compliant and weak, leading to a low effective stiffness in the transverse direction for the composite (Refs. 1 and 8). Furthermore, when a laminated unidirectional composite is loaded transverse to the fiber direction or in an off-axis direction, the initial mode of failure is fiber/matrix debonding, which leads to a sudden ultimate failure of the composite (Ref. 8). However, one cannot easily determine directly by experimental means the stiffness and strength properties of the interface. Therefore, to determine the stiffness of the interface, one needs to correlate the value based on the transverse stiffness of the unidirectional composite, since the transverse modulus of the composite is driven by the interfacial stiffness. The transverse modulus of the interface was therefore adjusted until the computed value of the axial modulus of the [90°] laminate matched the experimental value. The axial stiffness of the interface can be set to the transverse stiffness, since the interface has a minor contribution to the axial stiffness of the composite and assuming the interface is an isotropic material simplifies the analysis. The shear stiffness of the interface was computed using the usual assumptions of an isotropic material. To determine the transverse strength of the interface, a correlation based on the ultimate transverse strength of the composite was performed. The transverse strength of the interface was adjusted until the computed value of the ultimate transverse strength of the composite (the axial strength of the [90°] laminate) was equal to the experimental value. The axial strength of the interface was set equal to the transverse strength by assuming the interface is isotropic. The shear strength of the interface was assumed to be equal to the axial strength divided by the square root of three (again, a von Mises type of assumption for an isotropic material (Ref. 9)). The coefficient of thermal expansion used in Reference 1 was again applied here. The stiffness and strength properties for the interface are also given in Table 1.

Analysis Results

The effective elastic moduli for the SiC/RBSN $[0°]_8$, $[90°]_8$, $[10°]_8$, $[45°]_8$, $[0°_2/90°_2]_s$ and $[+45_2/-45_2]_s$ laminates described above were computed using MAC/GMC and are listed in Table 2. In addition, the effective shear modulus for the [0°] laminate was computed and is also shown in the table. The experimental values obtained in Reference 8 are also listed, including the statistical scatter. While the computed modulus for the [90°] laminate is a correlation, the remaining modulus values are predictive. Note that the initial correlation for the [90°] composite was carried out for an initial analysis of the stiffness response using a rudimentary micromechanics model. Since the interface stiffness utilized in the initial study still resulted in a reasonable, while not perfect, value for the [90°] modulus for the MAC/GMC unit cell used for this study, the correlation process was not repeated. In general, the comparison between the experimental and computed results was close to if not within the experimental

statistical scatter, demonstrating the MAC/GMC software can successfully compute the effective stiffness properties of laminated ceramic matrix composites.

The effective longitudinal stress-strain response for each of the laminates was also computed. The results for the $[0°]_8$, laminate are shown in Figure 3, the results for the $[90°]_8$ laminate are shown in Figure 4, the results for the $[10°]_8$ laminate are shown in Figure 5, the results for the $[45°]_8$ laminate are shown in Figure 6, the results for the $[0°_2/90°_2]_s$ laminate are shown in Figure 7, and the results for the $[+45_2/–45_2]_s$ laminate are shown in Figure 8. In all cases, the computed results are compared to the experimental results obtained in Reference 8. The computed and experimental stress levels at which the stress-strain curves for each of the laminates deviate from linearity are shown in Table 3, and the computed and experimental stress levels at which ultimate failure occurs are shown in Table 4. Note that for the $[90°]_8$, $[10°]_8$, and $[45°]_8$ laminates the experimental stress-strain curves displayed a sudden brittle failure which result in the ultimate stress being equal to the stress level at which the stress-strain curve deviates from linearity.

Examining the results for the [0°] laminate shown in Figure 4 (with the numerical values shown in Tables 3 and 4), the first matrix cracking stress is well correlated. After the matrix cracking took place, the computed stress level displayed a sudden jump downward followed by a continual increase in stress until final failure occurred. The primary cause for this stress jump is related to the simple subcell damage and failure model that was utilized for this study. Here, once the matrix subcells failed, the subcell instantaneously lost all of its stiffness and could not support any stress (given the strain controlled loading that was applied). The fact that the experimental stress-strain curve was more or less continuous indicates that in the actual composite the matrix can still hold stress, at least for some period of time, even after damage initiates. Another, secondary cause for the discrepancy between the experimental and analytical results is related to the fact that the response of ceramic matrix composites is known to be highly stochastic (Refs. 2 and 4). In the analyses conducted for this paper, amplified by the fact that only one unit cell was used, spatial statistical variation of the matrix strength was not taken into account. In the actual material response, with some areas of the matrix being stronger or weaker than others (possibly due to uneven distributions of porosity), the matrix failure is most likely more gradual, leading to a more gradual softening of the actual material stress-strain curve. This concept is hinted at in the actual material data shown by Bhatt and Phillips (Ref. 8), where at the point of the first matrix cracking stress the stress-strain curve displayed some “serrations” (not shown in the curve in Fig. 3), indicating that there was local matrix failure taking place in multiple locations at different times during the loading, until the entire matrix had failed. In the deterministic analyses conducted here, all of the matrix failed at one time. If the actual coupon utilized in the experiments was simulated with a spatially statistical variation of the matrix strength applied, the serrations observed in the experimental stress-strain curve might be observed. Future efforts will include the developed of improved progressive damage and failure models which will allow for subcells to continue to hold stress even after the initial point of damage and to allow for a gradual unloading of the stresses. After all the matrix fails, the secondary slope of the stress-strain curve, due primarily to the response of the fibers, is predicted well and the ultimate failure stress is well correlated. The fact that the secondary part of the stress-strain curve, if extended back to the zero strain point, would not show a zero stress indicates that the residual stresses are being applied correctly.

Examining the results for the [90°] laminate shown in Figure 4 (with the numerical values shown in Tables 3 and 4), the analysis predicted that the interface failed due to normal stresses at the experimental ultimate stress, as expected. However, in the experimental tests, once the interfacial failure occurred composite failure happened almost immediately (Ref. 8). In the computed results, a downward stress jump occurred followed by an increase in stress with a reduced slope until an ultimate failure, well above the experimental failure stress, occurred due to matrix failure. Relating to the unit cell diagram shown in Figure 2, at the point of interfacial failure the rows of subcells which included the interface were assigned a reduced stiffness and could then carry a negligible amount of stress. However, the row of subcells consisting of pure matrix still was able to carry stress after the interfacial failure, reflected in the continuing stress-strain curve. This result is confirmed by examining the secondary slope of the stress-

strain curve, which is equal to the matrix modulus scaled by the volume percentage of the matrix only row of the unit cell. Furthermore, the ultimate failure of the composite predicted by the analysis was due to failure in the matrix, that is in the matrix only row of the unit cell. In the actual composite, once the interfacial failure occurred, stress concentrations most likely formed and cracks propagated, leading to a sudden brittle failure. These forms of damage initiation and propagation cannot be modeled with the simple subcell failure models available within the current version of MAC/GMC. As mentioned earlier, future efforts will involve the development and implementation of more sophisticated subcell damage and failure models which can more accurately represent the actual behavior in the composite.

The computed stress-strain curve for the [10°] laminate (Fig. 5 and Tables 3 and 4) matches the experimental results fairly well. The ultimate stress is slightly overpredicted, while within the statistical scatter, but the sudden brittle failure of the laminate observed experimentally is captured. Interfacial shear failure was the first failure mode observed in the analytical results, followed almost immediately thereafter by matrix shear failure in the matrix only layers. These results indicate that in the actual composite failure most likely was also a result of the interface and matrix failing simultaneously.

For the [45°] laminate (Fig. 6 and Tables 3 and 4), at a stress level of approximately 57 MPa the analysis results predicted interfacial normal failure. This stress level is somewhat higher than, but within the statistical scatter of, the experimental failure stress. However, the stress level then dropped and the predicted global failure occurred due to shear failure in the matrix in the matrix only row of the subcell. This stress level was closer to the experimental failure stress, but the experimental results indicated a sudden brittle failure, which was not what was predicted. The inability of the analysis to predict a sudden brittle failure of the composite is most likely, once again, due to the simple subcell damage/failure model used. The reason that the predicted interfacial failure stress was somewhat higher than the experimental failure stress may be related to the use of a maximum stress failure criterion. If some form of interactive stress criterion was applied, the combination of normal and shear stresses in the interface may have been sufficiently high to cause failure at lower stress levels. Future efforts may involve examining additional failure criteria.

To examine the ability of MAC/GMC to predict the response of more complex laminate orientations, the computed stress-strain response of a $[0°/90°]_s$ laminate was determined and is shown in Figure 7 (numerical values in Tables 3 and 4). At a stress level of approximately 80 MPa, interfacial failure in the 90° plies was predicted, but only a relatively small change in the computed stress-strain curve occurred. The experimental stress-strain showed no noticeable nonlinearity in the material at this point. Furthermore, Bhatt and Phillips (Ref. 8) found that no damage was present at stress levels below 100 MPa, at which point cracking occurred mostly in the [0°] layers, with some cracking occasionally seen in the [90°] layers. These observations for the most part correlate with what was predicted analytically. The significant first matrix cracking stress observed experimentally was nicely predicted (well within the statistical scatter), and was computed to be the result of matrix failure in the 0° plies. The stress dip after the first matrix cracking stress was predicted once again, and was most likely due to the same factors as were discussed in the discussion of the [0°] laminate analyses. The ultimate stress was overpredicted and the secondary slope after the first matrix cracking stress was overpredicted, to a level above the statistical scatter. However, both Murthy, et al. (Ref. 1) and Bhatt and Phillips (Ref. 8) also encountered these results in their analyses of the data, and could not come up with a good reason for the discrepancy. In both previous studies it was concluded that fiber damage must have occurred in the actual composite, leading to the lower secondary slope, which was not captured analytically.

The stress-strain response of a [+45°/–45°] laminate was also computed and is shown in Figure 8 (numerical values in Tables 3 and 4). The analysis results predicted sudden brittle failure, starting with interfacial shear failure followed by matrix shear failure, at a stress level somewhat below the first matrix cracking stress determined experimentally (and outside of the statistical scatter). Furthermore, the fact that the experimental stress-strain curve continued after the first matrix cracking stress occurred was not captured by the analysis, indicating that in the actual composite there is some interaction of the stresses occurring which is not being captured by the analysis. Furthermore, in the actual composite interfacial

failure may not have occurred. As discussed by Bhatt and Phillips (Ref. 8), above the initiation of nonlinearity only matrix damage occurred and was localized to relatively small regions of the specimens, indicating that the damage observed experimentally was much lower than what was predicted. Future efforts will attempt to determine the reason for these discrepancies.

Conclusions

The Generalized Method of Cells micromechanics method and the MAC/GMC software code were used to determine the effective mechanical response of the SiC/RBSN laminated ceramic matrix composite for various laminate orientations. Methods were developed to characterize the constituent properties based on a combination of experimental data at the constituent level combined with correlations based on the composite level response. The stiffness properties of the composite were predicted relatively well. The first matrix cracking stress and ultimate strength of the composite, as well as the longitudinal stress-strain response of laminates with various fiber orientations were predicted to various levels of accuracy. The deficiencies between the experimental and computed results were primarily due to the use of a relatively simple damage/failure model. Secondarily, the use of purely deterministic and not statistical material properties, and possibly an inaccurate application of residual stresses may have also been a factor. All of these deficiencies can be addressed in future efforts. However, the results shown in this paper indicate that the MAC/GMC software has a great deal of potential to provide a needed analysis capability in the design of structures composed of ceramic matrix composites.

References

1. Murthy, P.L.N., C.C. Chamis, and S.K. Mital. 1996. "Computational Simulation of Continuous Fiber-Reinforced Ceramic Matrix Composite Behavior," NASA Technical Paper 3602, National Aeronautics and Space Administration, Washington, D.C.
2. Lamon, J., 2001. "A micromechanics-based approach to the mechanical behavior of brittle-matrix composites," *Composites Science and Technology*, 61:2259-2272.
3. Mital, S.K, B.A. Bednarcyk, S.M. Arnold and J. Lang. 2009. "Modeling of Melt-Infiltrated SiC/SiC Composite Properties," NASA/TM—2009-215806, National Aeronautics and Space Administration, Washington, D.C.
4. Liu, K.C. and S.M. Arnold. 2011. "Impact of Material and Architecture Model Parameters on the Failure of Woven Ceramic Matrix Composites (CMCs) Via the Multiscale Generalized Method of Cells," NASA/TM—2011-217011, National Aeronautics and Space Administration, Washington, D.C.
5. Paley, M. and J. Aboudi. 1992. "Micromechanical Analysis of Composites by the Generalized Method of Cells," *Mechanics of Materials* 14:127–139.
6. Pindera, M.-J. and B.A. Bednarcyk. 1999. "An efficient implementation of the generalized method of cells for unidirectional, multi-phased composites with complex microstructures," *Composites: Part B*, 30:87-105.
7. Bednarcyk, B.A. and S.M. Arnold. 2002. "MAC/GMC 4.0 User's Manual - Keywords Manual," NASA/TM-2002-212077/VOL2, National Aeronautics and Space Administration, Washington, D.C.
8. Bhatt, R.T. and R.E. Phillips. 1990. "Laminate Behavior for SiC Fiber-Reinforced Reaction-Bonded Silicon Nitride Matrix Composites," *Journal of Composites Technology and Research*, 12(1):13-23.
9. Chen, W.-F. and Han, D.-J. 2007. *Plasticity for Structural Engineers*. J. Ross Publishing. pp. 77-78.

TABLE 1.—CONSTITUENT PROPERTIES

Constituent	Modulus, GPa	Poisson ratio	Coefficient of thermal expansion (m/m/°C)	Axial strength, MPa
Fiber	390	0.17	4.1	2250
Matrix	110	0.22	2.2	84
Interface	1.8	0.22	2.0	32

TABLE 2.—PREDICTION OF STIFFNESS PROPERTIES

Fiber orientation	Axial modulus-experimental (GPa) (Ref. 8)	Axial modulus-computed, (GPa)	Shear modulus-experimental (GPa) (Ref. 8)	Shear modulus-computed, (GPa)
[0]	193±7	190	31±2	28.5
[90]	69±3	73.3	--------	--------
[10]	165.3±4	168.8	--------	--------
[45]	81.81±5	77.26	--------	--------
[0/90]	124±6	132.1	--------	--------
[±45]	78±3	82.56	--------	--------

TABLE 3.—PREDICTION OF FIRST MATRIX CRACKING/NONLINEAR STRESS

Fiber orientation	Measured stress, (MPa) (Ref. 8)	Computed stress, (MPa)
[0]	227±41	231.81
[90]	27±3	28.58
[10]	162±34	176.24
[45]	43±17	57.48
[0/90]	127±26	132.17
[+45/–45]	75±10	60.27

TABLE 4.—PREDICTION OF GLOBAL FAILURE STRENGTH

Fiber orientation	Measured stress, (MPa) (Ref. 8)	Computed stress, (MPa)
[0]	682±150	676.29
[90]	27±3	35.47
[10]	162±34	176.24
[45]	43±18	40.78
[0/90]	294±87	338
[+45/–45]	100±16	60.269

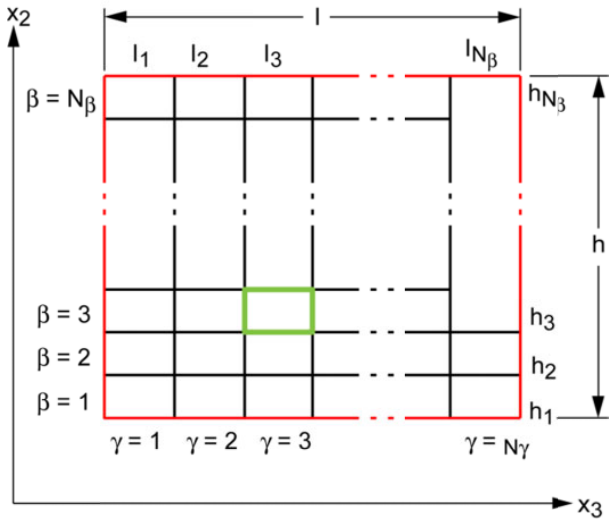

Figure 1.—Repeating unit cell subcell discretization for generalized method of cells (Ref. 7).

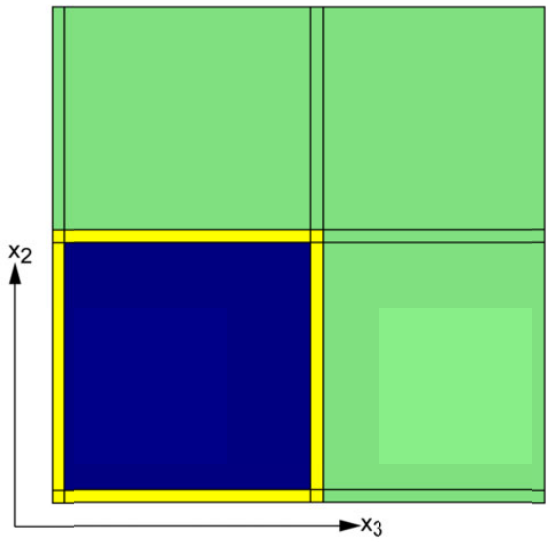

Figure 2.—MAC/GMC unit cell used for analysis (not to scale).

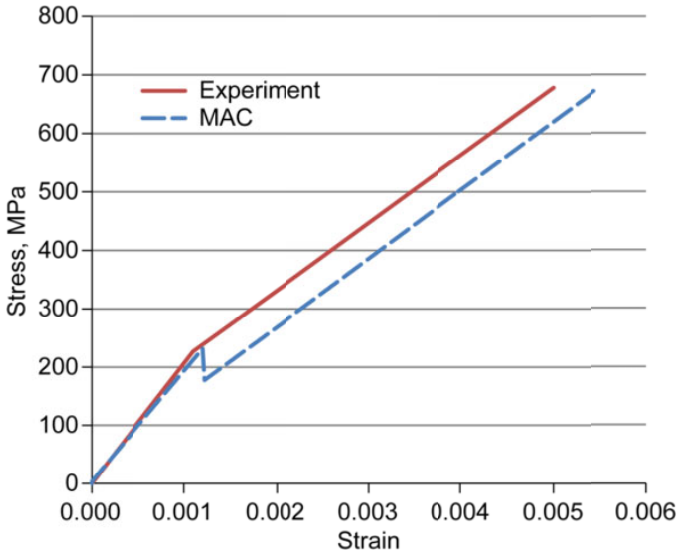

Figure 3.—Experimental and computed stress-strain curves for [0°] SiC/RBSN laminate.

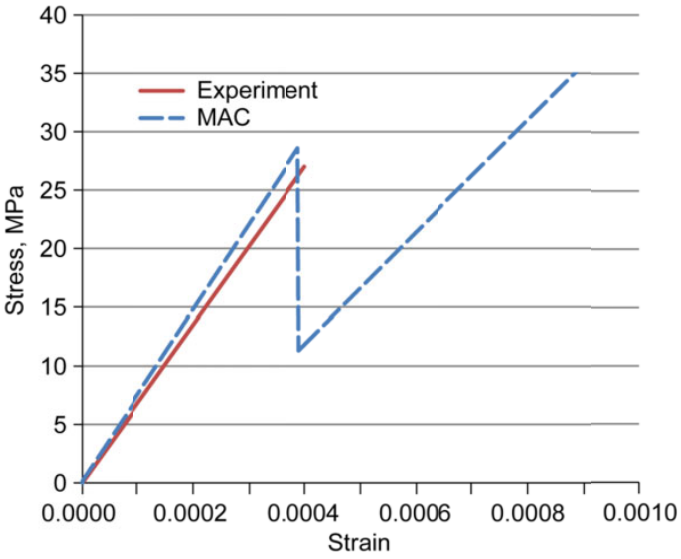

Figure 4.—Experimental and computed stress-strain curves for [90°] SiC/RBSN laminate.

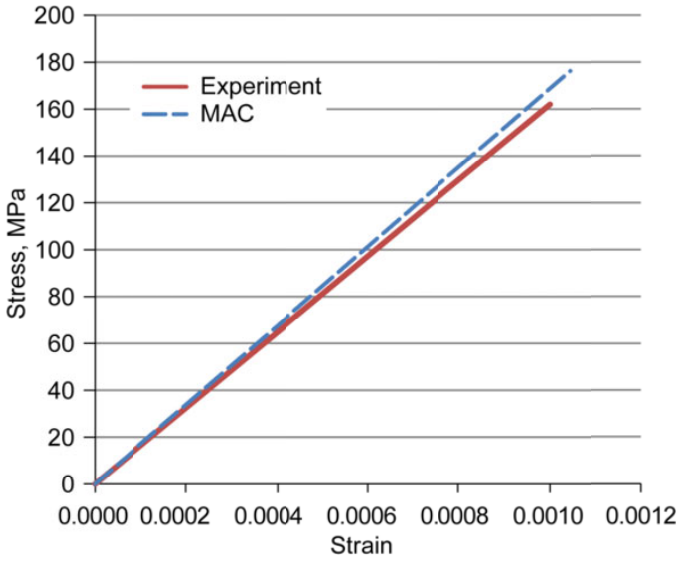

Figure 5.—Experimental and computed stress-strain curves for [10º] SiC/RBSN laminate.

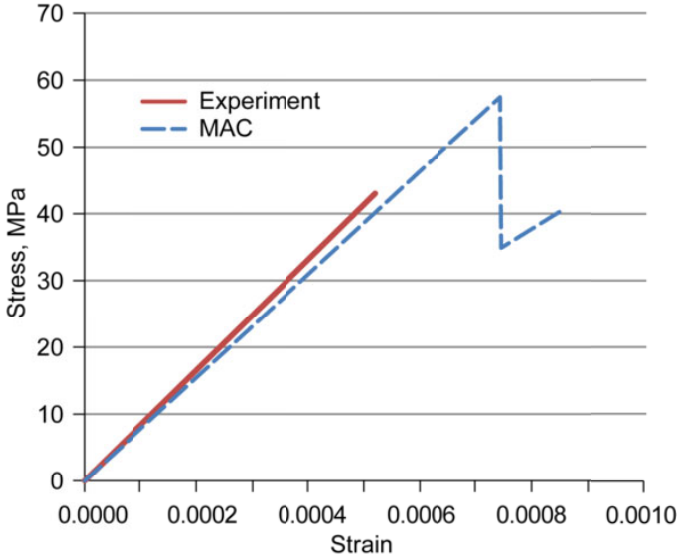

Figure 6.—Experimental and computed stress-strain curves for [45º] SiC/RBSN laminate.

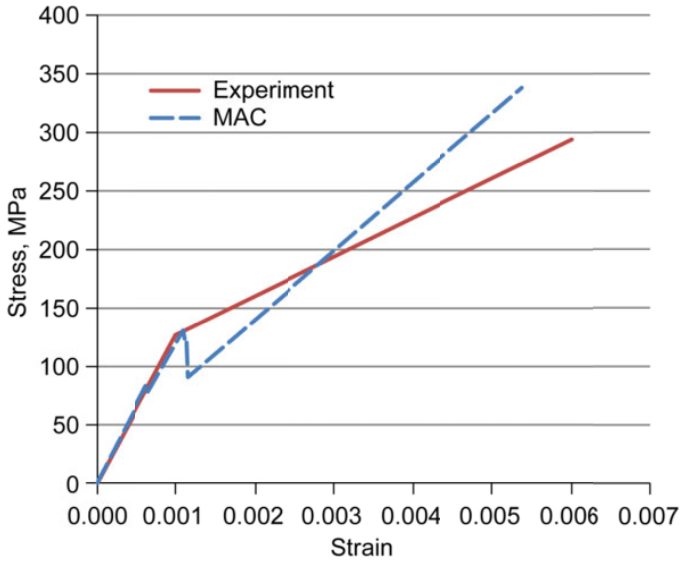

Figure 7.—Experimental and computed stress-strain curves for $[0°/90°]_S$ SiC/RBSN laminate.

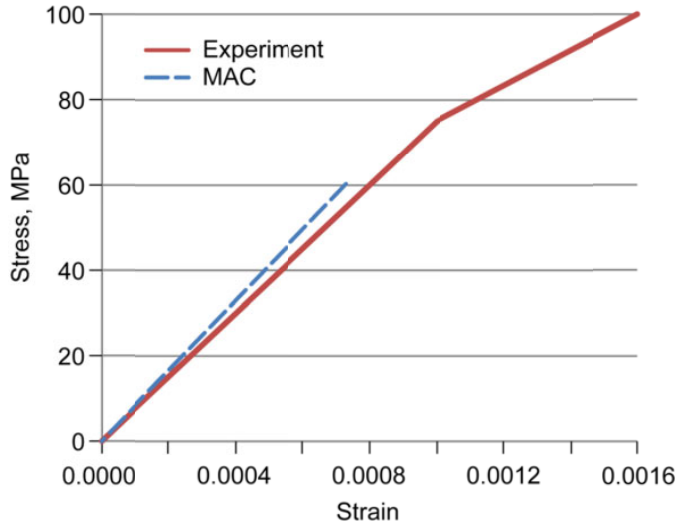

Figure 8.—Experimental and computed stress-strain curves for $[+45°/–45°]_S$ SiC/RBSN laminate.

REPORT DOCUMENTATION PAGE	Form Approved OMB No. 0704-0188

1. REPORT DATE *(DD-MM-YYYY)*	2. REPORT TYPE	3. DATES COVERED *(From - To)*
01-10-2012	Technical Memorandum	

4. TITLE AND SUBTITLE
Utilization of the Generalized Method of Cells to Analyze the Deformation Response of Laminated Ceramic Matrix Composites

5a. CONTRACT NUMBER

5b. GRANT NUMBER

5c. PROGRAM ELEMENT NUMBER

6. AUTHOR(S)
Goldberg, Robert, K.

5d. PROJECT NUMBER

5e. TASK NUMBER

5f. WORK UNIT NUMBER
WBS 984754.02.07.03.16.03.02

7. PERFORMING ORGANIZATION NAME(S) AND ADDRESS(ES)
National Aeronautics and Space Administration
John H. Glenn Research Center at Lewis Field
Cleveland, Ohio 44135-3191

8. PERFORMING ORGANIZATION REPORT NUMBER
E-18482

9. SPONSORING/MONITORING AGENCY NAME(S) AND ADDRESS(ES)
National Aeronautics and Space Administration
Washington, DC 20546-0001

10. SPONSORING/MONITOR'S ACRONYM(S)
NASA

11. SPONSORING/MONITORING REPORT NUMBER
NASA/TM-2012-217737

12. DISTRIBUTION/AVAILABILITY STATEMENT
Unclassified-Unlimited
Subject Categories: 24 and 39
Available electronically at http://www.sti.nasa.gov
This publication is available from the NASA Center for AeroSpace Information, 443-757-5802

13. SUPPLEMENTARY NOTES

14. ABSTRACT
In order to practically utilize ceramic matrix composites in aircraft engine components, robust analysis tools are required that can simulate the material response in a computationally efficient manner. The MAC/GMC software developed at NASA Glenn Research Center, based on the Generalized Method of Cells micromechanics method, has the potential to meet this need. Utilizing MAC/GMC, the effective stiffness properties, proportional limit stress and ultimate strength can be predicted based on the properties and response of the individual constituents. In this paper, the effective stiffness and strength properties for a representative laminated ceramic matrix composite with a large diameter fiber are predicted for a variety of fiber orientation angles and laminate orientations. As part of the analytical study, methods to determine the in-situ stiffness and strength properties of the constituents required to appropriately simulate the effective composite response are developed. The stiffness properties of the representative composite have been adequately predicted for all of the fiber orientations and laminate configurations examined in this study. The proportional limit stresses and strains and ultimate stresses and strains were predicted with varying levels of accuracy, depending on the laminate orientation. However, for the cases where the predictions did not have the desired level of accuracy, the specific issues related to the micromechanics theory were identified which could lead to difficulties that were encountered that could be addressed in future work.

15. SUBJECT TERMS
Ceramic matrix composites; Micromechanics

16. SECURITY CLASSIFICATION OF:			17. LIMITATION OF ABSTRACT	18. NUMBER OF PAGES	19a. NAME OF RESPONSIBLE PERSON
a. REPORT	b. ABSTRACT	c. THIS PAGE			STI Help Desk (email:help@sti.nasa.gov)
U	U	U	UU	20	19b. TELEPHONE NUMBER *(include area code)* 443-757-5802